



Cite this: *Chem. Commun.*, 2019, 55, 10124

Received 9th June 2019,  
Accepted 26th July 2019

DOI: 10.1039/c9cc04415a

[rsc.li/chemcomm](http://rsc.li/chemcomm)

## Uniform lithium deposition on N-doped carbon-coated current collectors†

Na Zhang,  <sup>a</sup> Seung-Ho Yu  <sup>\*ab</sup> and Héctor D. Abruña  <sup>\*a</sup>

**A Cu foil current collector was coated with polydopamine-derived nitrogen-doped carbon (N-C) to regulate Li nucleation and growth. The lithium nucleation overpotential was significantly lowered, and Li was deposited in a spherical morphology without dendrites, dramatically improving the Li plating/stripping coulombic efficiency.**

In order to meet the ever-increasing energy demands and reduce the global dependence on fossil fuels, it is urgent to develop electrical energy storage systems for renewable energies.<sup>1</sup> Lithium-ion batteries (LIBs) have brought a revolution to this landscape since their commercialization in 1991 by Sony Corp. For the past decades, tremendous efforts have been devoted to improving the performance of LIBs.<sup>2</sup> However, the capacity provided by LIBs, limited by their intrinsic reaction mechanisms, is not sufficient to meet growing requirements.<sup>2,3</sup> Next generation rechargeable batteries, including Li-S batteries and Li-O<sub>2</sub>, emerged as advanced battery systems and have attracted enormous attention, because of their high capacity, low cost, earth abundance and environmental friendliness.<sup>4,5</sup> The operation of these batteries requires the use of metallic Li as the anode, which is also believed to be the ultimate anode material for rechargeable batteries. This is because Li has an ultrahigh theoretical capacity of 3810 mA h g<sup>-1</sup> and the lowest negative electrochemical potential (-3.04 V vs. the standard hydrogen electrode), making it the highest energy density anode.<sup>6</sup> However, the commercialization of lithium metal anodes has not been achieved to date. This is due to a variety of reasons including the low coulombic efficiency, infinite relative volumetric change and the severe growth of lithium dendrites.<sup>7</sup> Particularly, the uncontrolled formation of Li dendrites can not only give rise to "dead Li" which leads to fast capacity loss,

but also poses severe safety concerns by penetrating the separator and causing an internal short circuit.<sup>7,8</sup>

To tackle these obstacles, various approaches have been proposed, including developing solid-state electrolytes to prevent dendrite formation by mechanical means,<sup>9-11</sup> modification of the electrolyte concentration and additives to stabilize the SEI layer,<sup>12-14</sup> and construction of porous matrices to accommodate lithium.<sup>15,16</sup> Various carbon materials have been widely studied and employed as conductive lithium hosts.<sup>17-19</sup> In order to render carbon lithiophilic for homogeneous lithium deposition with lower nucleation overpotentials, doping strategies have been proposed.<sup>20</sup> Nitrogen-doped graphene was found to guide Li nucleation and suppress lithium dendrite formation, increasing its coulombic efficiency.<sup>21</sup> Designing host materials for Li deposition can prevent the growth of lithium dendrites, however, the construction of these hosts usually involves complex procedures, which are not suitable for industrial manufacturing and scale-up. Introducing inactive host materials will also decrease the specific gravimetric and volumetric energy densities of the batteries. Therefore, controlling the lithium deposition on a traditional anode current collector, Cu foil, is of great significance for the large-scale and economic-effective production of lithium metal anodes. However, much less effort has been focused on the modification of lithiophilic Cu foils.

Herein, we report on a facile method to regulate lithium nucleation and growth by coating Cu foil with a thin layer of nitrogen-doped carbon, which was derived from the carbonization of polydopamine as a carbon precursor. The lithiophilic nitrogen-doped carbon on the Cu foil can significantly reduce the nucleation overpotential and effectively suppress the formation of lithium filaments. The morphology of the plated Li on the Cu foil coated with nitrogen-doped carbon (N-C) was spherical, in contrast to the needle-like dendrites formed on the bare Cu foil. In addition, due to the efficient inhibition of Li dendrites, the coulombic efficiencies of lithium stripping/plating were dramatically improved at both high current densities and high areal capacities.

<sup>a</sup> Baker Laboratory, Department of Chemistry and Chemical Biology, Cornell University, Ithaca, New York, 14853, USA. E-mail: [hda1@cornell.edu](mailto:hda1@cornell.edu)

<sup>b</sup> Department of Chemical and Biological Engineering, Korea University, 145 Anam-ro, Seongbuk-gu, Seoul 02841, Republic of Korea. E-mail: [seunghoy@korea.ac.kr](mailto:seunghoy@korea.ac.kr)

† Electronic supplementary information (ESI) available: Experimental methods. See DOI: 10.1039/c9cc04415a

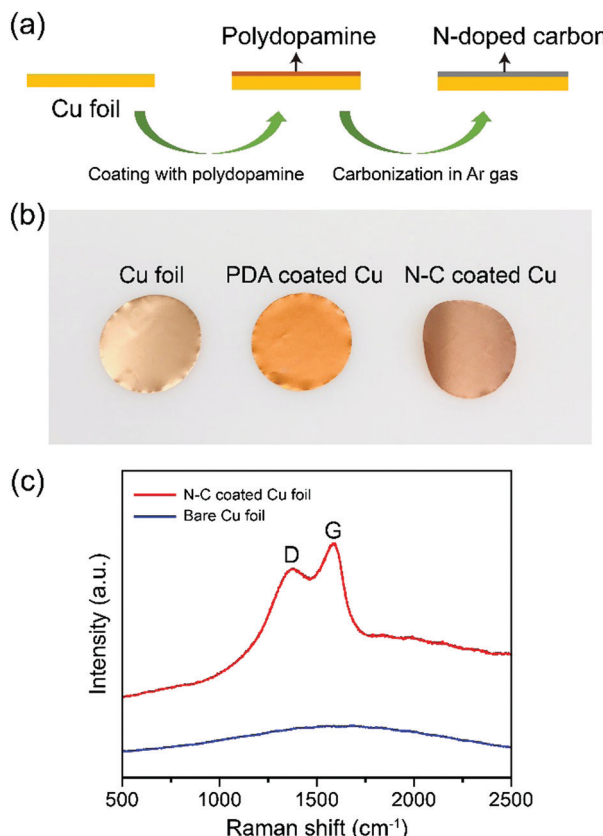


Fig. 1 (a) Schematic illustration of the coating process on the surface of a Cu foil with a layer of nitrogen-doped carbon. (b) The color change of the surface on the Cu foil at each coating stage. (c) Raman spectra of a bare Cu foil and a nitrogen-doped carbon coated Cu foil.

Coating with polydopamine is an easy and versatile method for modifying surfaces.<sup>22</sup> Thus, a commercial anode current collector, Cu foil, was initially coated with polydopamine *via* polymerization of dopamine on the surface. The coated foil was carbonized in an inert atmosphere (Ar) to produce the nitrogen-doped carbon. The coating process of the Cu foil is illustrated by the scheme in Fig. 1a and the color of the Cu foil at each coating stage can be seen in Fig. 1b, which shows that the Cu surface turns darker after the carbonization process. The Raman spectrum of the N-C coated Cu foil, in Fig. 1c, clearly presents two peaks at  $1350\text{ cm}^{-1}$  and  $1585\text{ cm}^{-1}$ , corresponding to the characteristic D and G bands of carbon, respectively. This demonstrates that the surface of the Cu foil was coated with carbon, derived from the polydopamine. A scanning electron microscope (SEM) image (Fig. S1a, ESI<sup>†</sup>) shows that after coating with the N-C layer, the surface is flat, and the cross-sectional transmission electron microscope (TEM) image (Fig. S1b, ESI<sup>†</sup>) clearly shows that the thickness of the N-C layer is around 5–10 nm. X-ray photoelectron spectroscopy (XPS) N 1s spectrum of the N-C coated Cu confirms the presence of pyridinic and pyrrolic nitrogen (Fig. S2, ESI<sup>†</sup>). Several reports have demonstrated that N-doped carbons are lithiophilic and can control the Li nucleation and growth.<sup>20,21,23</sup> Therefore, it is reasonable to posit that the N-C coated Cu foil

could suppress the Li dendrite growth and improve the cycling performance.

To probe the Li nucleation process on the bare Cu foil and the N-C coated Cu foil, half cells were assembled by employing a bare Cu or N-C coated Cu foil as a working electrode and a Li foil as the counter/reference electrode in a carbonate-based electrolyte (1 M LiPF<sub>6</sub> in EC/DEC). By applying a constant current density for a specified period of time, a desired amount of Li could be deposited on the current collector. The nucleation overpotential for Li is an important parameter for evaluating the lithiophilicity of the surface of the current collector. Fig. 2a shows the charge–discharge voltage profiles of Li deposition on the bare Cu and N-C coated Cu foils at a current density of  $1\text{ mA cm}^{-2}$ . The lithium nucleation overpotential is determined from the difference between the initial voltage drop and the subsequent flat voltage plateau. Li deposited on the bare Cu foil exhibited a nucleation overpotential of  $\sim 313\text{ mV}$  at a current density of  $1\text{ mA cm}^{-2}$ . In contrast, at the same current density, the N-C Cu foil exhibited a much smaller nucleation overpotential of  $\sim 219\text{ mV}$ . In addition, the flat voltage plateau at  $-80\text{ mV}$  on the N-C coated Cu foil, which corresponds to the mass-transfer overpotential, affected by Li migration, was much lower than at the bare Cu foil ( $-115\text{ mV}$ ). The diminished

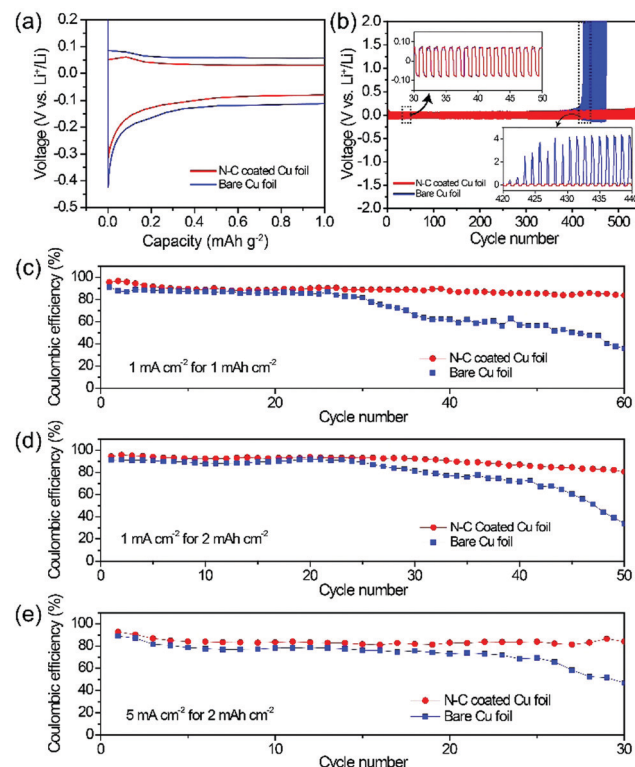


Fig. 2 (a) Galvanostatic charge/discharge voltage profiles for a bare Cu foil and a N-C coated Cu foil at a current density of  $1\text{ mA cm}^{-2}$ . (b) The cycling performance of symmetric cells using the Li deposited on a bare Cu foil and a N-C coated Cu foil as a working electrode. The coulombic efficiency of Li stripping/plating for the bare Cu foil and N-C coated Cu foil (c) at a current density of  $1\text{ mA cm}^{-2}$  with a capacity of  $1\text{ mA h cm}^{-2}$ , (d) at a current density of  $1\text{ mA cm}^{-2}$  with a capacity of  $2\text{ mA h cm}^{-2}$ , and (e) at a current density of  $5\text{ mA cm}^{-2}$  with a capacity of  $2\text{ mA h cm}^{-2}$ .

nucleation overpotential is largely due to the lithiophilic N-doped carbon coating, lowering the resistance for lithium to nucleate and plate on the surface.

The long-term cycling stability of the deposited Li was studied in a symmetric Li/Li cell. A pre-stored Li capacity of  $4.0 \text{ mA h cm}^{-2}$  was initially plated on the bare Cu foil or N-C coated Cu foil, which were used as working electrodes, and commercial Li foils were used as the counter/reference electrodes. The cells were subsequently cycled at a current density of  $1 \text{ mA cm}^{-2}$  with a capacity of  $0.042 \text{ mA h cm}^{-2}$ . As shown in Fig. 2b, Li on the N-C coated Cu foil exhibited a much longer cycling stability. In the beginning, the overpotential of Li stripping from the bare Cu foil is similar to that of the N-C coated Cu foil (see inset of Fig. 2b). However, after about 420 cycles, the overpotential for the bare Cu foil electrode increased dramatically, so that less and less lithium could be stripped off from the electrode. In contrast, the overpotential for the N-C coated Cu foil remained stable for over 550 cycles. This reflects an improved stability of the Li deposited on the N-C coated Cu foil, which is likely due to much lower formation of "dead Li".<sup>24</sup>

The coulombic efficiency, defined as the capacity ratio of Li stripping to plating, is also a critical factor to evaluate the performance of metallic Li anodes.<sup>25,26</sup> Efficiency tests were conducted in half cells with bare Cu or N-C coated Cu foils as the working electrode. The cells were initially cycled at a low current density of  $50 \mu\text{A cm}^{-2}$  in a voltage window of  $0\text{--}1 \text{ V}$  for 3 cycles to stabilize the SEI layer and remove contaminants.<sup>27</sup> As shown in Fig. 2c and d, the coulombic efficiency of the N-C Cu foil stabilized at 90% after over 50 cycles at a current density of  $1 \text{ mA cm}^{-2}$ , while the efficiency of the bare Cu foil fell below 70% after 35 cycles and 40 cycles, for capacities of  $1 \text{ mA h cm}^{-2}$  and  $2 \text{ mA h cm}^{-2}$ , respectively. More significantly, high current density measurements are important for practical operation of lithium metal batteries. Therefore, the coulombic efficiency was further tested at the high current density of  $5 \text{ mA cm}^{-2}$  with a high capacity of  $2 \text{ mA h cm}^{-2}$ . As shown in Fig. 2e, the efficiency for the N-C coated Cu foil was higher and more stable than that for the bare Cu foil. This indicates that the nitrogen-doped carbon enables a stable cycling performance with improved coulombic efficiencies at both high current densities and high capacities, suggesting the feasibility for practical applications. It should be noted that in this work, we employed a corrosive carbonate-based electrolyte without any additives. Thus, much higher improvements can be expected when employing ether-based electrolytes, such as 1,3-dioxolane and 1,2-dimethoxyethane (DOL/DME), or electrolyte additives (e.g., fluoroethylene carbonate).<sup>28</sup>

The greatly enhanced performance is ascribed to the lithiophilic nitrogen-doped carbon which can not only regulate the lithium nucleation, but also suppress the growth of lithium dendrites. The morphology of the Li deposits was studied by scanning electron microscopy (SEM) as shown in Fig. 3a-d. Lithium was plated on the bare Cu or N-C coated Cu at a current density of  $1 \text{ mA cm}^{-2}$  for a capacity of  $0.25 \text{ mA h cm}^{-2}$ . As shown in Fig. 3a and b, the lithium deposited on the bare Cu foil clearly exhibits the formation of filamentous structures with lengths of a few micrometers at the nucleation stage.

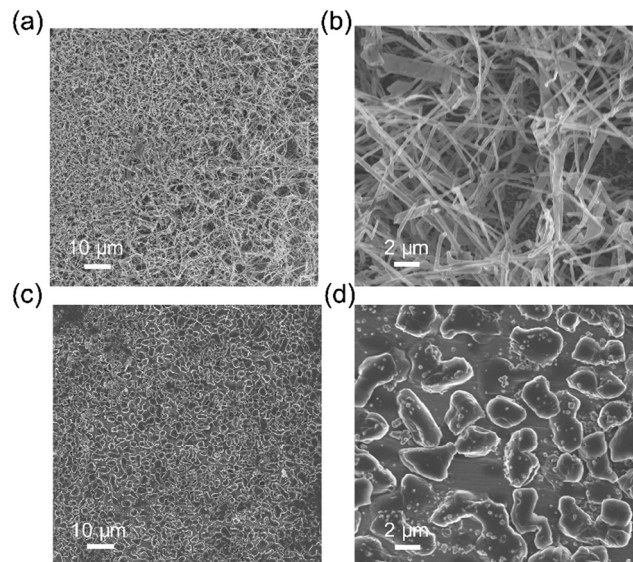


Fig. 3 The SEM images of the lithium deposited on the bare Cu foil at (a) low magnification and (b) high magnification. The morphology of Li deposits on the N-doped carbon coated Cu foil at (c) low magnification and (d) high magnification.

For the N-C coated Cu foil (Fig. 3c and d), there were no dendrites formed, but instead, large spherical Li particles with a size of  $2\text{--}10 \mu\text{m}$  were observed, indicating the effective control of Li plating. As reported, initial homogenous Li nucleation can also regulate the following uniform Li growth.<sup>29</sup> Therefore, efficient suppression of Li dendrites can be realized by the nitrogen-doped carbon layer on the surface of Cu foil, as shown in Fig. S3 (ESI†).

The Li nucleation behaviors on a bare Cu foil and a N-C coated Cu foil are illustrated in Fig. 4. When a bare Cu foil is employed as the current collector, the nucleation sites for Li are random and Li prefers to nucleate at the protuberances, resulting in non-uniform Li deposition. In addition, the surface of the Cu foil is not lithiophilic, making the Li nucleation barrier so high that Li is more likely to grow on the pre-existed

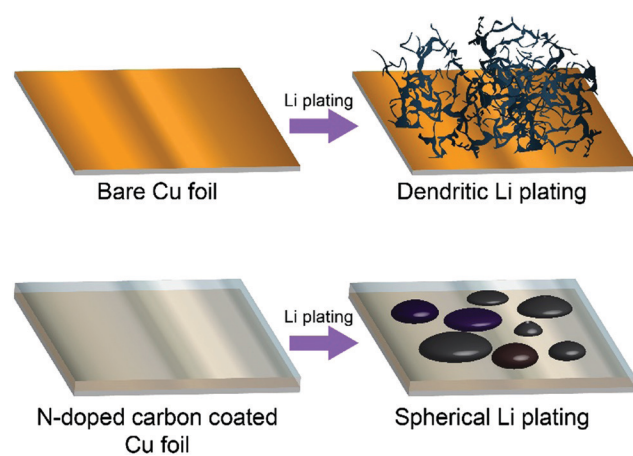


Fig. 4 Schematic representation of the Li nucleation and growth on the bare Cu foil (top) and the N-doped carbon coated Cu foil (bottom).

deposits,<sup>21</sup> leading to the fast formation of lithium dendrites. In contrast, for the N-C coated Cu foil, the nitrogen-doped carbon coating layer is lithiophilic with a much lower Li nucleation overpotential, than on the bare Cu foil. Thus, Li can deposit uniformly on the surface of the N-C coated Cu foil and yield homogeneous deposits without dendrite formation. The successful inhibition of lithium dendrite growth could ensure a stable cycling performance for Li stripping/platting, by avoiding the increased surface area induced by the dendrites and preventing the fast consumption of the electrolyte.

In summary, a surface modified current collector, Cu foil, coated with a nitrogen-doped carbon film was obtained by carbonizing polydopamine. The homogeneous lithiophilic N-doped carbon layer was effective in controlling the nucleation process of Li and suppressing the growth of Li dendrites. By lowering the nucleation overpotential, N-C promotes the uniform formation of spherical Li particles instead of Li filaments. As a result, the coulombic efficiency of Li stripping/platting on the N-C Cu foil exhibited great improvements at both high current densities and high capacities. The long-term cycling stability of symmetric cells was also significantly enhanced due to the dendrite-free morphology and reduced side reactions. This work demonstrates that the coating strategy of the anode current collector, Cu foil, with a lithiophilic material, N-doped carbon, is an effective method to suppress Li dendrite growth and is also cost-effective for large-scale production.

This work made use of the Cornell Center for Materials Research (CCMR) Shared Facilities with funding from the NSF MRSEC program (DMR-1719875). The authors thank E. Padgett and D. A. Muller for the help with transmission electron microscope measurements.

## Conflicts of interest

There are no conflicts to declare.

## Notes and references

- 1 J.-M. Tarascon and M. Armand, *Nature*, 2001, **414**, 359–367.
- 2 J. B. Goodenough and Y. Kim, *Chem. Mater.*, 2010, **22**, 587–603.
- 3 S.-H. Yu, X. Feng, N. Zhang, J. Seok and H. D. Abruña, *Acc. Chem. Res.*, 2018, **51**, 273–281.

- 4 P. G. Bruce, S. A. Freunberger, L. J. Hardwick and J.-M. Tarascon, *Nat. Mater.*, 2011, **11**, 172.
- 5 N. Zhang, B. D. A. Levin, Y. Yang, D. A. Muller and H. D. Abruña, *J. Electrochem. Soc.*, 2018, **165**, A1656–A1661.
- 6 X. B. Cheng, R. Zhang, C. Z. Zhao and Q. Zhang, *Chem. Rev.*, 2017, **117**, 10403–10473.
- 7 P. Albertus, S. Babinec, S. Litzelman and A. Newman, *Nat. Energy*, 2017, **3**, 16–21.
- 8 W. Xu, J. Wang, F. Ding, X. Chen, E. Nasybulin, Y. Zhang and J.-G. Zhang, *Energy Environ. Sci.*, 2014, **7**, 513–537.
- 9 Q. Zheng, L. Ma, R. Khurana, L. A. Archer and G. W. Coates, *Chem. Sci.*, 2016, **7**, 6832–6838.
- 10 Q. Zheng, D. M. Pesko, B. M. Savoie, K. Timachova, A. L. Hasan, M. C. Smith, T. F. Miller, G. W. Coates and N. P. Balsara, *Macromolecules*, 2018, **51**, 2847–2858.
- 11 J. Li, C. Ma, M. Chi, C. Liang and N. J. Dudney, *Adv. Energy Mater.*, 2015, **5**, 1401408.
- 12 S.-H. Yu, X. Huang, J. D. Brock and H. D. Abruña, *J. Am. Chem. Soc.*, 2019, **141**, 8441–8449.
- 13 J. Zheng, P. Yan, D. Mei, M. H. Engelhard, S. S. Cartmell, B. J. Polzin, C. Wang, J.-G. Zhang and W. Xu, *Adv. Energy Mater.*, 2016, **6**, 1502151.
- 14 Y. Liu, D. Lin, Y. Li, G. Chen, A. Pei, O. Nix, Y. Li and Y. Cui, *Nat. Commun.*, 2018, **9**, 3656.
- 15 Q. Yun, Y. B. He, W. Lv, Y. Zhao, B. Li, F. Kang and Q. H. Yang, *Adv. Mater.*, 2016, **28**, 6932–6939.
- 16 L. L. Lu, J. Ge, J. N. Yang, S. M. Chen, H. B. Yao, F. Zhou and S. H. Yu, *Nano Lett.*, 2016, **16**, 4431–4437.
- 17 Y. Wang, Y. Shen, Z. Du, X. Zhang, K. Wang, H. Zhang, T. Kang, F. Guo, C. Liu, X. Wu, W. Lu and L. Chen, *J. Mater. Chem. A*, 2017, **5**, 23434–23439.
- 18 T. T. Zuo, X. W. Wu, C. P. Yang, Y. X. Yin, H. Ye, N. W. Li and Y. G. Guo, *Adv. Mater.*, 2017, **29**, 1700389.
- 19 S. Liu, A. Wang, Q. Li, J. Wu, K. Chiou, J. Huang and J. Luo, *Joule*, 2018, **2**, 184–193.
- 20 X. Chen, X. R. Chen, T. Z. Hou, B. Q. Li, X. B. Cheng, R. Zhang and Q. Zhang, *Sci. Adv.*, 2019, **5**, eaau7728.
- 21 R. Zhang, X. R. Chen, X. Chen, X. B. Cheng, X. Q. Zhang, C. Yan and Q. Zhang, *Angew. Chem., Int. Ed.*, 2017, **56**, 7764–7768.
- 22 J. H. Ryu, P. B. Messersmith and H. Lee, *ACS Appl. Mater. Interfaces*, 2018, **10**, 7523–7540.
- 23 L. Liu, Y. X. Yin, J. Y. Li, S. H. Wang, Y. G. Guo and L. J. Wan, *Adv. Mater.*, 2018, **30**, 1706216.
- 24 K. N. Wood, E. Kazyak, A. F. Chadwick, K.-H. Chen, J.-G. Zhang, K. Thornton and N. P. Dasgupta, *ACS Cent. Sci.*, 2016, **2**, 790–801.
- 25 J. C. Burns, A. Kassam, N. N. Sinha, L. E. Downie, L. Solnickova, B. M. Way and J. R. Dahn, *J. Electrochem. Soc.*, 2013, **160**, A1451–A1456.
- 26 B. D. Adams, J. Zheng, X. Ren, W. Xu and J.-G. Zhang, *Adv. Energy Mater.*, 2018, **8**, 1702097.
- 27 C. P. Yang, Y. X. Yin, S. F. Zhang, N. W. Li and Y. G. Guo, *Nat. Commun.*, 2015, **6**, 8058.
- 28 X. Wang, W. Zeng, L. Hong, W. Xu, H. Yang, F. Wang, H. Duan, M. Tang and H. Jiang, *Nat. Energy*, 2018, **3**, 227–235.
- 29 A. Pei, G. Zheng, F. Shi, Y. Li and Y. Cui, *Nano Lett.*, 2017, **17**, 1132–1139.